Powder Metallurgy Progress, Vol.18 (2018), No.2, p.080-095
http://dx.doi.org/10.1515/pmp-2018-0009

STUDYING THE PROGRESS OF SINTERING IN FERROUS POWDER COMPACTS BY IN-SITU MEASURING THE THERMAL CONDUCTIVITY

H. Danninger, G. Leitner, Ch. Gierl-Mayer

Abstract

In situ characterization of the sintering process is a difficult task, in particular for systems without pronounced dimensional changes. Dilatometry is not too helpful in those cases, and therefore other properties have to be recorded. In the present study, sintering of ferrous powder compacts was studied in situ by measuring the thermal diffusivity ***a*** *using a laser flash apparatus. This property is a measure to characterise the heat flow through a material; it depends on the contact area between the particles and thus reveals their change during sintering. It is shown that the change of* ***a*** *during sintering of ferrous compacts is much less pronounced than in the case of cemented carbides which is not surprising when regarding the widely differing porosity changes. The results are however in good agreement with expectations when considering some experimental limitations. The trend for the thermal conductivity λ. which can be calculated from* ***a****, the specific heat and the density, is in good agreement with that found for the electrical conductivity, both properties being linked through Wiedemann-Franz' law.*

Keywords: Sintered steels; sintering; in-situ characterization; laser flash; thermal diffusivity

INTRODUCTION

Both for scientific research and for stable and reliable industrial production, the basic processes occurring during the sintering cycle have to be known. The traditional route to study sintering is to perform runs under varying parameters such as temperature, time and atmosphere and then cooling or quenching the specimens with subsequent investigation such as mechanical testing, metallography etc. This can be done as stepwise sintering or through interrupted runs. These indirect methods however give only indirect information about the progress of sintering; a result is obtained but is cannot immediately be stated during which step of sintering this result has been obtained. Furthermore, e.g. for simulating the sintering process the properties at a given temperature are of relevance and have to be known [1].

Herbert Danninger, Christian Gierl-Mayer: Technische Universität Wien, A-1060 Wien/Vienna, Austria
Gert Leitner: retired; formerly Fraunhofer-Institut für Keramische Technologien und Systeme (IKTS), D-01277 Dresden, Germany

Direct characterization of sintering is decidedly more informative. So far, mainly the various methods of thermal analysis such as dilatometry [2], thermogravimetry, differential thermal analysis/scanning calorimetry, in part combined [3] and also linked to chemical analysis such as mass spectrometry [4], have been used. These methods give valuable insight into dimensional changes, enthalpy changes, and chemical reactions occurring during sintering. However they do not yield information about microstructural changes such as formation and growth of sintering contacts. An interesting approach has been made by Shoales [5] who measured the strength of specimens in various stages of the sintering process and could find relationships to distortion. However, each measurement consumes one specimen. For studying the distortion, also optical methods have been applied [6], but these just give the macroscopic results but not so much the microstructural background.

For studying the formation and growth of sintering contacts e.g. in PM steels, measuring the electrical conductivity $\boldsymbol{\kappa}$ has been proposed quite early, both from the as sintered samples [7] and also in-situ (e.g. Ritzau, in [8]). Conductivity is quite directly linked to the effective load bearing cross section that controls most of the properties [9-12], and measuring the conductivity in-situ would be an attractive method to follow the sintering process. However, $\boldsymbol{\kappa}$ is fairly difficult to measure in-situ mainly due to contacting problems at elevated temperatures, the contacts inevitably exhibiting temperature gradients that affect the resistivity of the system in a rather unpredictable way. As shown by Simchi et al., the change of conductivity is most pronounced in the early stages of sintering while especially in the later stages of isothermal sintering, changes are marginal [10-12]. Therefore, characterization of electrical (or thermal) conductivity seems to be particularly suited for the heating section of the sintering cycle which however, as stressed by Schatt [13], is of high relevance for the entire sintering process.

For metallic materials, $\boldsymbol{\kappa}$ is linked to the thermal conductivity $\boldsymbol{\lambda}$ through Wiedemann-Franz' law, i.e.

$$\lambda/\kappa = k.T \qquad (1)$$

k being a constant of about 2.44E-8 $V^2.K^{-2}$ [14]. I.e. measuring the thermal conductivity should give information about the microstructural changes as well as measuring the electrical conductivity.

Measuring the thermal conductivity in situ at elevated temperatures is also tricky, but the thermal diffusivity $\boldsymbol{a}$ – which is linked to $\boldsymbol{\lambda}$ by the relationship

$$\boldsymbol{a} = \lambda/\rho.c_p \qquad (2)$$

can be more easily measured using modern equipment, and measurement of c_p is routine in thermal analysis now, as is the change of the density with temperature through dilatometry.

Today, determination of the thermal diffusivity through the laser flash method is a quite mature technique and can be regarded as a reliable tool for standard materials. It has been applied e.g. for studying the sintering of ceramics, in part combined with other thermoanalytical methods [15]. In this case, sintering is linked to pronounced densification, typically full density being targeted with high performance ceramic materials. On the other hand, it could not be taken for granted that laser flash can be properly used also for porous metal bodies that markedly change their microstructure during sintering – i.e. also during the measuring routine – but not so much their total porosity, as characteristic for sintered steels used for PM precision parts,.

In the present study, in-situ sintering of compacts prepared from plain iron, Fe-C as well as Mo and Cr-Mo prealloy steels has been studied using the laser flash technique. Prealloyed powders were used to avoid effects of alloy element homogenization [16, 17] which would also affect the conductivity (see e.g. [18]). The sintering behaviour of these materials had already been studied in detail through conventional techniques, using e.g. interrupted sintering runs with subsequent characterization of the specimens [19-21]. The reliability of the laser flash measurements could thus at least qualitatively be checked.

EXPERIMENTAL PROCEDURE AND MATERIALS

Powder compacts were prepared from water atomized powders, iron powder ASC 100.29 and prealloyed steel powders Astaloy Mo and Astaloy CrM being used (all supplied by Höganäs AB, Sweden). In part natural graphite (Kropfmühl UF4) was admixed. The compositions tested are given in Table 1. The powder batches were mixed in a tumbling mixer (except for the plain iron powder) and uniaxially compacted to form billets with 16 mm diameter and about 5 mm thickness. The compacting pressure was set at 500 MPa, and die wall lubrication was afforded using Multical sizing fluid. The samples were pressed with a diameter significantly larger than the diameter of the sample holder (12.6 mm) to compensate for (improbable but possible) geometrical changes of the specimens by shrinkage during sintering.

Tab.1. Characteristics of the powder compacts used for in-situ measurements.

Code	Starting powder	$C_{nominal}$ [mass %]	Cr [mass %]	Mo [mass %]	Fe	Green density [$g.cm^{-3}$]
#1	ASC 100.29	-	-	-	Balance	6.97
#2	ASC 100.29	0.8	-	-	Balance	6.88
#3	Astaloy1.5Mo	0.8	-	1.5	Balance	6.89
#4	AstaloyCrM	0.8	3.0	0.5	Balance	6.71

The thermal diffusivity was measured using a laser flash apparatus Netzsch LFA 427 supplied by Netzsch Geraetebau GmbH (Selb, Germany). This equipment uses an Nd-YAG-Laser (pulse duration 0.5 ms; the temperature increase by the laser pulse is < 2 K). Details of the measuring technique are described in [22, 23].

The specimens were inserted into the vacuum chamber of the laser flash tester, and then the chamber was evacuated to a pressure of $<10^{-3}$ mbar. Since the laser flash apparatus requires stable thermal conditions, heating of the specimens had to be done stepwise. At each selected temperature, three parallel measurements of the thermal diffusivity were done while holding the temperature of the sample constant. After the three shots, the sample was heated up to the next selected temperature with a heating rate of 10 K/min. The whole procedure can be characterized by an average heating or cooling rate of about 3 K/min. Each run was done in a heating and cooling ramp, and a second (parallel) run was performed immediately after the first one, in order to study the microstructural changes caused by the first thermal cycle. The maximum temperature was set at 1000°C for both the first and the second cycle.

At temperatures above 200°C, the uncertainty of measurement regarding the values of thermal diffusivity is less than 5 %. At lower temperatures larger uncertainties exist because of a reduced sensitivity of the infrared detector. The temperature uncertainty is about 5 K (heating) ... 10 K (cooling).

The specific heat capacity c_p was measured by standard DSC technique calibrated with sapphire standards. Pressed samples were investigated in a heat flux DSC 404 supplied

by Netzsch Gerätebau GmbH (Selb / Germany). The measurements were done in high purity argon (99.999%) with a heating rate of 20 K/min. The uncertainty of measurement regarding the values of specific heat capacity is less than 10 %. The temperature uncertainty is about 1 K.

In Figure 1 the microstructures of the materials investigated are shown; to simulate the state of the laser flash specimens after the runs, impact test bars were prepared at the same conditions, i.e. pressed at 500 MPa and sintered following the same cycle; as atmosphere, the high purity air was used. As can be seen, the microstructures are fairly coarse, which is evident both with plain Fe and the carbon containing steels and is not surprising due to the very slow cooling. In the case of plain Fe, coarsening is further enhanced by the transformation effect described e.g. in [24, 25]. Furthermore, the fraction of ferrite is rather high considering the carbon content, which is particularly noticeable with Fe-0.8%C; also this can be attributed to the slow cooling which enhances formation of ferrite. Of course also some carbon loss must be considered occurring by reaction with the natural oxygen content of the metal powders.

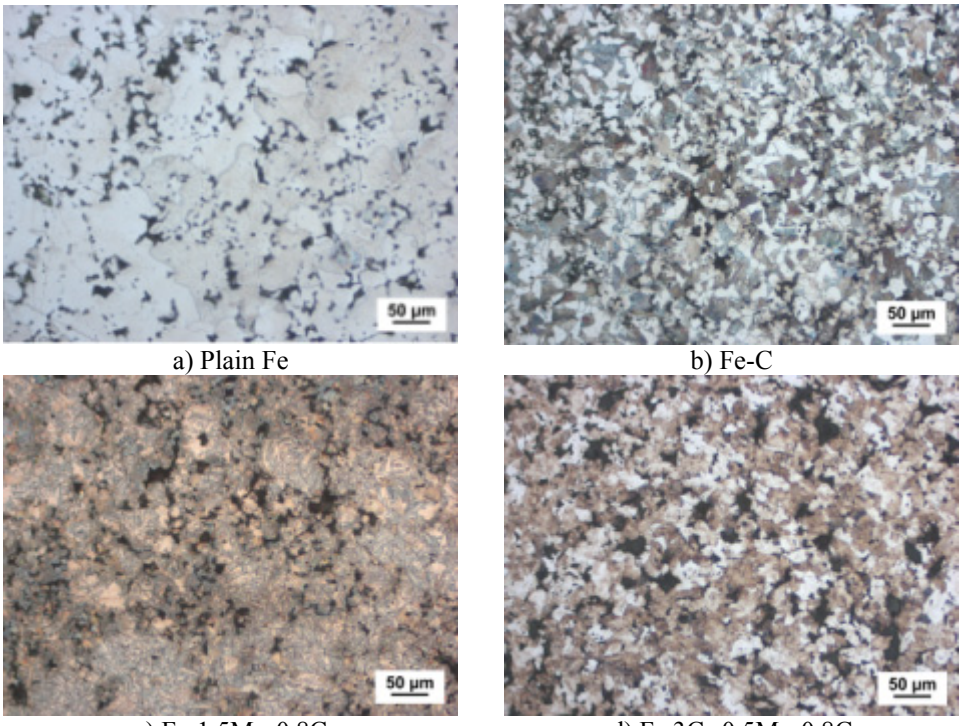

a) Plain Fe b) Fe-C

c) Fe-1.5Mo-0.8C d) Fe.3Cr-0.5Mo-0.8C

Fig.1. Microstructures of powder compacts sintered in Ar following the same sintering profile as in the laser flash device.

EXPERIMENTAL RESULTS – IN-SITU LASER FLASH TESTS

The thermal diffusivity data obtained for plain iron are given in Fig.2 as a function of the temperature for the first (Fig.2a) and the second run (Fig.2b). Parallel runs with other specimens yielded virtually identical results, which indicates that the reproducibility of the method is highly satisfactory. As can be clearly seen there are considerable differences

between the heating and cooling sections in the first run while in the second run the results for heating and cooling are virtually identical. This confirms that those changes of the microstructure that are relevant for affecting the thermal diffusivity occur virtually exclusively during the first heating stage; after this stage the microstructural changes do not have any noticeable effect on the thermal diffusivity (at least unless the maximum temperature of the first run is not exceeded in the second run). This indicates that the processes influencing the thermal diffusivity are predominantly temperature-controlled (as are also e.g. the degassing phenomena in sintered steels, see [20, 26]). This further implies that the stepwise heating mode that is necessary for the laser flash experiments should not yield markedly different results from those that would be obtained in case of continuous heating with the same integral heating rate.

From the comparison of the heating and cooling stages in the first run it is further clear that the primary differences are found in the low temperature range, i.e. below approx. 600°C, which agrees well with the results given by Simchi et al. for the electrical conductivity [10, 11]. Generally the changes of the thermal diffusivity are not too pronounced, both with regard to the temperature effect – the spread here being from 0.04 to 0.21 $cm^2.s^{-1}$ maximum – and from the material, the differences between the green compact and that after the second run being in the range of less than 1:2 which indicates that in green compacts pressed with die wall lubrication the thermal diffusivity – and also the conductivity – is not too low, which also agrees with the findings of Simchi et al. for the electrical conductivity [10, 11] who found that for die wall lubricated compacts the increase of the conductivity is less pronounced than for compacts with admixed lubricants since also the initial level, i.e. $\boldsymbol{\kappa}$ of the compacts, is much higher in the former case, due to the absence of insulating organic substances in the pressing contacts.

Addition of carbon to the metal powders results in a further component the particles of which are located especially in the pressing contacts of the green compact (and of course also in the pores, which however should not be of much effect here). The respective graphs thermal diffusivity vs. temperature for the plain carbon steel Fe-0.8%C are given in Fig.3. Here it stands out quite clearly that the differences between the graphs for the heating and cooling sections, respectively, are markedly more pronounced than in the case of the plain iron compacts (Fig.2a). In particular the low temperature section of the heating graphs exhibits markedly lower $\boldsymbol{a}$ values. This may be attributed to the fact that graphite is less conducting (both for heat and electricity) than is metal, and the graphite flakes enclosed in the pressing contacts thus exert an effect on the conductivity that is more pronounced than that of the very thin oxide layers covering the iron particles, which furthermore are to some extent penetrated during pressing.

On the other hand, the decrease of $\boldsymbol{a}$ in the temperature range RT .. 400°C which is particularly pronounced in the case of the plain iron (from 0.12 to 0.04 $cm^2.s^{-1}$) is much smaller with the Fe-C compact with regard both to the absolute and the relative drop of the thermal diffusivity. Since the drop in the thermal diffusivity of the matrix metal should be the same for plain iron and iron-carbon (the graphite not yet being dissolved in the latter) it must be concluded that there is a relative improvement in the "quality" of the contacts, and here it can be assumed that the cleaning of the particle surfaces due to desorption of adsorbed gases and the decomposition of hydroxides is more pronounced in the case of graphite containing materials since it has been shown that apparently a considerable fraction of the compounds that are removed in the first part of the sintering process (up to about 400°C) originates from the graphite (see [26]). This cleaning of the surface results in an increased thermal diffusivity which in part compensates for the drop of $\boldsymbol{a}$ in the base metal.

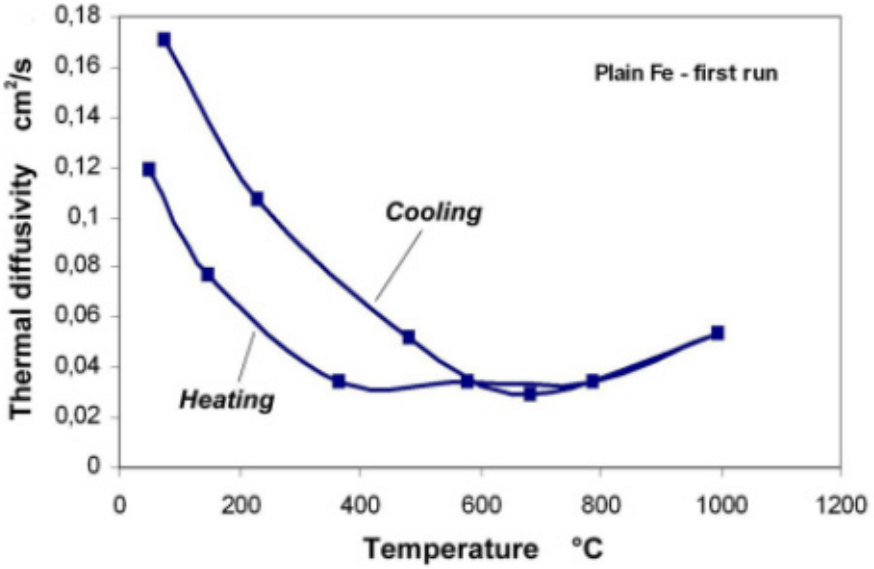

a) First run

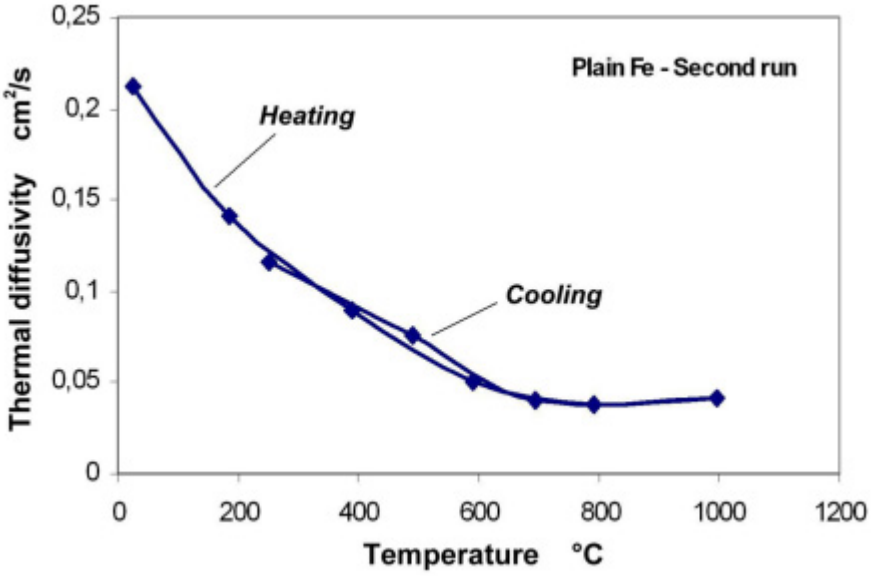

b) Second run

Fig.2. Thermal diffusivity of plain iron as a function of the temperature during a sintering run up to 1000°C. Atomized iron powder, compacted at 500 MPa, vacuum.

The cooling graph shows the same trend as that of plain iron, indicating that this behaviour is controlled by the behaviour of the matrix material, although the level of ***a*** remains lower (due to the different, i.e. two-phase microstructure). Also here, as in the case of plain iron, no effect of the α-γ phase transformation – which for Fe-C occurs at significantly lower temperatures than for Fe - is discernible in the graphs.

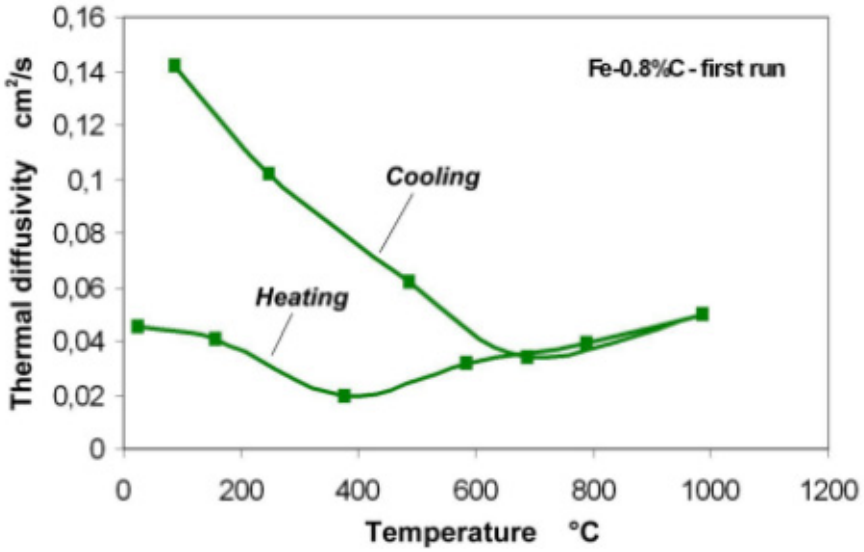

Fig.3. Thermal diffusivity of Fe-0.8%C as a function of the temperature during a sintering run up to 1000°C. Atomized iron powder, compacted at 500 MPa, vacuum.

As stated above, the alloy steels containing Mo and Cr-Mo, respectively, were prepared from prealloyed powders, and therefore no homogenisation effects – except of course of carbon – should occur. The graphs are shown in Fig.4. Here it stands out clearly that the trend is quite similar to that observed with the Fe-C material, i.e. compared to plain iron a rather low initial value for the thermal diffusivity but also a rather slight drop towards higher temperatures.

A typical feature is the fact that with both materials the virtual overlap of the heating and cooling graphs in the temperature range 600…1000°C is not discernible any more but that the increase of ***a*** in the heating section is more pronounced than the decrease in the cooling branch. This effect is particularly characteristic for the higher alloyed steel Fe-3%Cr-0.5%Mo-C but can be seen to some extent also with Fe-1.5%Mo-C. The Cr alloy steel however does not exhibit the typical steady increase of ***a*** between 600 and 1000°C but there is only one large step between 800 and 1000°C. Here it must be kept in mind that according to Kremel et al. [19], reduction of the oxide layers covering the Fe-Cr-Mo prealloy particles takes place only at about 1000°C minimum while for Fe-C or also Fe-Mo-C this effect occurs at about 700 ... 800°C. As shown in [27], formation of stable sintering necks is possible only after the reduction process has occurred. Therefore it can be assumed that for the Cr-Mo steel the carbothermal reduction of the oxides at the maximum temperature of the measuring run has resulted in neck formation and an according increase of the thermal diffusivity while with the other steels the deoxidation occurs at much lower temperatures, and neck formation is thus governed rather by the onset of diffusion and not by a chemical reaction.

The cooling branches of the respective graphs are quite similar to those found in Fe and Fe-C; of course the absolute levels for the ***a*** values are again lower due to the effect of the dissolved alloy elements. However, this effect becomes more pronounced at lower temperatures, which agrees with the results described in [26] which showed that the effect of solid solution on the thermal conductivity decreases with higher temperatures and virtually disappears at T > 600°C while that of the porosity remains.

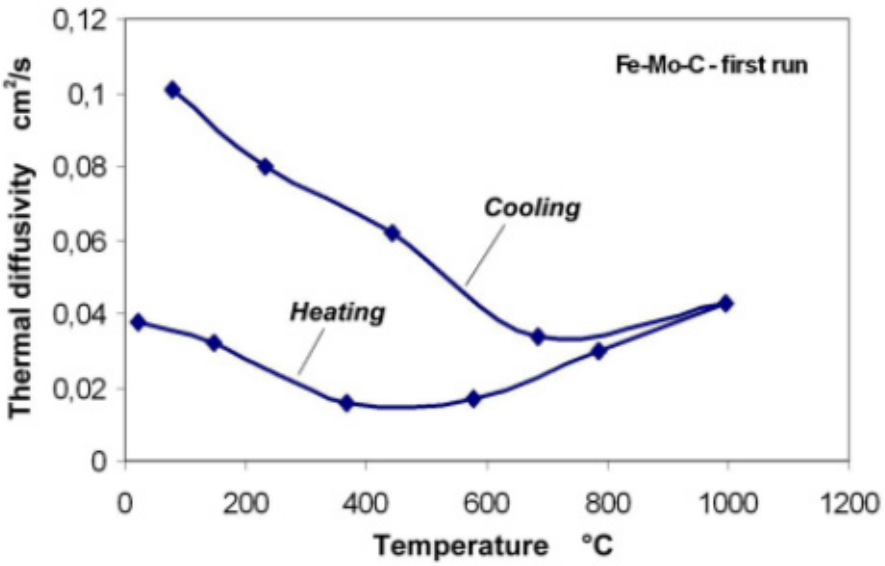

a) Fe-1.5%Mo-0.8%C

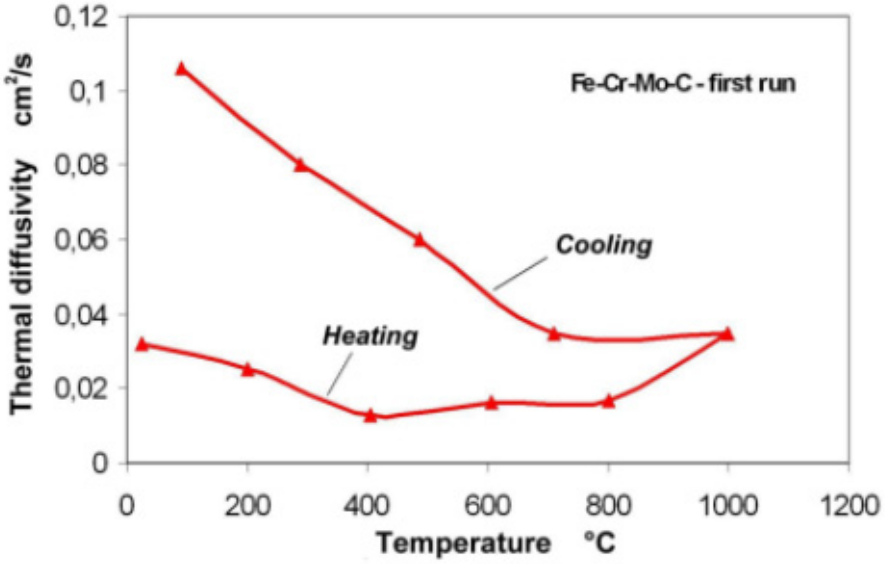

b) Fe3.0%Cr-0.5%Mo-0.8%C

Fig.4 Thermal diffusivity of alloy steels Fe-1.5%Mo-0.8%C and Fe-3%Cr-0.5%Mo-0.8%C as a function of the temperature during a sintering run up to 1000°C. Atomized prealloyed iron powder, compacted at 500 MPa, vacuum.

DISCUSSION

Thermal diffusivity measurements for in-situ characterization of the sintering process have been successfully used with cemented carbides. However, the sintering behaviour of PM ferrous compacts differs markedly from that of hardmetals (WC-Co, ...).

The latter are characterized by a pronounced densification during sintering, indicated by accordingly high shrinkage of typically 16 ... 18 % linear (similar to sintering of ceramics, see above). Shrinkage begins when oxidic impurities on the surfaces of the hard material particles (WC, ...) are reduced by the carbon of the mixture [29]. Only above these temperatures shrinkage takes place, caused by diffusion processes. Due to the same reasons the contact areas between the particles are cleaned and enlarged, and thus a better heat transfer through the porous sample is possible. In [30] it has been shown that a pronounced increase of thermal diffusivity and a similarly pronounced decrease of length coincide, starting at a temperature of 750 °C for a standard grain size hard metal WC-10 wt.% Co (DS 130 from HC Starck / Germany).

With ferrous PM compacts, on the other hand, the role of densification is rather marginal, and the improvement of the mechanical properties during sintering is almost exclusively due to changes in neck – i.e. in sintering contact – geometry while the total porosity remains practically unchanged. This results in much lower effect of sintering on thermal and mechanical properties, and it might therefore be assumed that the thermal conductivity/diffusivity is decidedly better suited for characterizing the sintering process of specimens the porosity of which changes drastically during sintering – hard metals, heavy alloys, MIM products – than sintering of ferrous parts.

However, also for the latter of course the increase in neck dimension and strength has some impact on the electrical and thermal properties. As shown quite early by Esper et al. [6], and later in more detail e.g. by Simchi [10-12] for the electrical conductivity, the effect of sintering is most pronounced in the early stages of the sintering process while e.g. a change of the sintering temperature from 1120° to 1250°C has only marginal effect on $\boldsymbol{\kappa}$.

The same phenomenon seems to hold also for the thermal properties, which is not surprising due to the close links between thermal and electrical conductivity of metallic materials. In order to assess if the results for $\boldsymbol{a}$ obtained in-situ through laser flash are in agreement with the conductivity/resistivity values obtained with the same type of materials by Simchi et al. [10-12], first the thermal conductivity $\boldsymbol{\lambda}$ was calculated according to Eq.2 from the $\boldsymbol{a}$ values obtained for plain iron. The density values for the various temperatures were taken from the literature [31] as were the values for the specific heat c_p [29, 30]; experimental measurements (see above) were found to be in good agreement with the literature data. As a reference, the data for fully dense plain iron were taken. The resulting values are given in Fig.5; also the relative thermal conductivity, i.e. that of the porous body normalized to that of fully dense material at the same temperature, is plotted there.

The striking similarity between the graphs for the porous and the dense materials and those plotted in Fig.1a is quite evident which indicates that in fact during the *cooling section* of the test run the thermal properties of the material are affected primarily by the matrix material rather than by changes of the pore structure or neck characteristics. In the *heating section*, on the other hand, the latter mechanisms seem to play a major role. The drop in the relative thermal conductivity between RT and 400°C is at first surprising, at least when taking into account the behaviour of the carbon containing steels in this temperature range (Fig.3); however it reflects the more pronounced drop of $\boldsymbol{a}$ in this temperature range observed with plain iron. One possible explanation might be that in plain iron there are no graphite particles which, though they are rather poor conductors, form bridges in the pressing contacts while in plain iron the removal of the volatile surface compounds – which are electrically insulating but nevertheless thermally conducting - tends to weaken the pressing contacts until the onset of sintering results in the formation of more stable bridges (see discussion below). In any case it is clearly evident that the main increase

of the relative conductivity occurs between 500 and 800°C, at least qualitatively quite similar to the effects of sintering reported for the electrical conductivity.

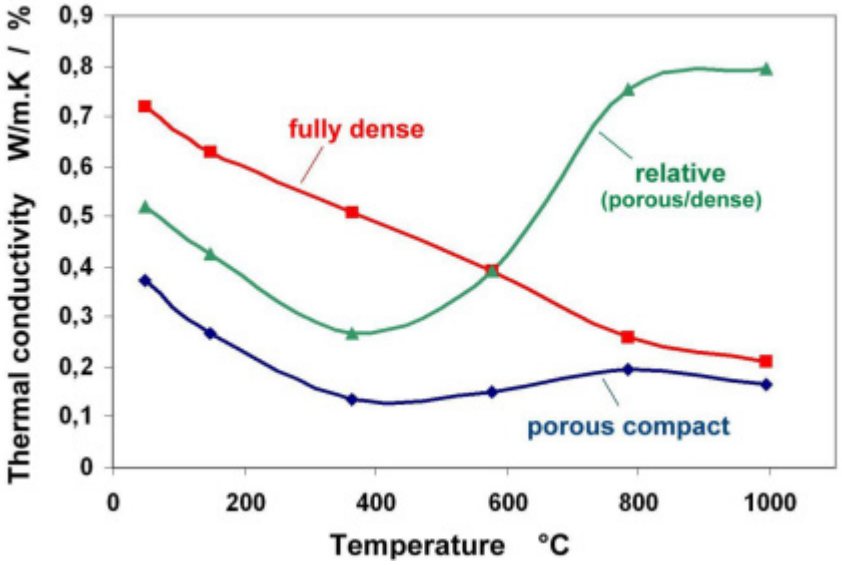

Fig.5. Thermal conductivity λ (calculated from a obtained through laser flash) of a porous plain iron compact (first heating) compared to the theoretical values for a fully dense body.

If the electrical resistivity of the plain iron specimens is calculated from the thermal conductivity using Wiedemann-Franz' law (Eq.1) the graphs given in Fig.6 are obtained. Due to the direct relationship the graph is virtually a reverse plot of that given in Fig.5 (though somewhat distorted by the effect of the temperature). For comparison, the resistivity of fully dense plain iron is also given. The almost parallel trend of the graphs of the cooling section and of the theoretical values for fully dense iron is evident, once more confirming that all changes of the pore structure and neck geometry have occurred in the heating section while during cooling only the resistivity of the matrix metal is of importance.

If the results obtained are compared to those given by Simchi et al. [10, 11] it stands out clearly that the initial resistivity, i.e. that of the green compact, calculated from laser flash data is much too low, being in the range of about 0.2×10^{-4} Ω.cm while Simchi gives values of $>50 \times 10^{-4}$ Ω.m for the green compact (pressed with die wall lubrication). On the other hand, after the cooling run the final resistivity is in very good agreement with Simchi's values, being in the range of about 0.15×10^{-4} Ω.m, while Simchi gives about 0.13×10^{-4} Ω.m.

This discrepancy can be explained by the fact that Wiedemann-Franz' law holds for metallic systems while initially the powder particles surfaces are covered by oxides, hydroxides, in part also lubricant, for which this correlation between electrical and thermal properties cannot be applied, the non-metallic layers being thermally conductive but not electrically, and calculating the electrical conductivity κ from the thermal one gives too high κ = too low resistivity. Only at a temperature at which the non-metallic layers have been removed to a considerable extent, i.e. when the metallic contacts dominate the

interfacial area between the powder particles, thermal and electrical conductivity tend to agree.

This means that if in-situ methods are to be used for assessing the formation and growth of metallic contacts, determination of the resistivity is better suited than that of the thermal conductivity / diffusivity since the latter is contributed to also by insulating layers that do not bear any load. On the other hand, measuring the thermal diffusivity through laser flash is fairly easy and not as sensitive to experimental problems while yielding quite interesting results at least for the low to moderate temperature range of sintering. At higher temperatures the heat transfer by radiation must be taken into account which takes place also through the pore space, and the role of the sintering contacts will probably be somewhat obscured.

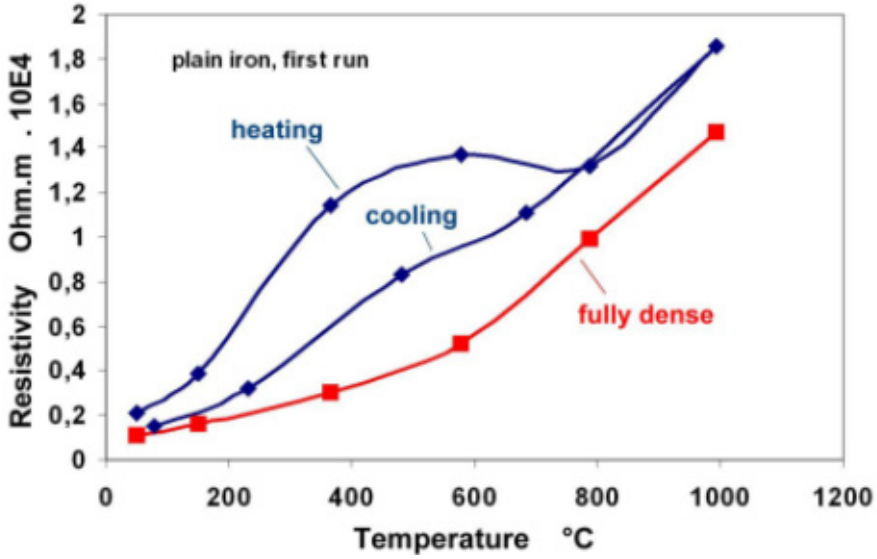

Fig.6. Resistivity of plain iron, calculated from the thermal diffusivity (first run, heating and cooling), as a function of the temperature.

When comparing the evolution of thermal diffusivity for the different materials investigated here, it is helpful to compare on one hand the heating section and on the other hand the cooling part separately. In Fig.7a, the heating section is shown for Fe and Fe-0.8%C. It is evident that, as stated above, at low temperatures, i.e. for the pressed compact, there is a pronouncedly lower diffusivity for the Fe-C specimen compared to Fe; however, the drop of ***a*** with higher temperatures is markedly less pronounced. At about 600°C the two graphs virtually merge, which is somewhat surprising insofar as it excludes graphite as the main reason for the lower ***a*** of the Fe-C materials: as shown e.g. in [20, 33], graphite is dissolved to a considerable degree only well above 800°C. It seems that the dissolution of graphite plays a much lower role towards the thermal diffusivity than the formation of the first metallic bridges. This is also evident from the fact that in the temperature range 800 …1000°C there is hardly any difference between Fe and Fe-C; if graphite played a major role, a significant change of a would be noticeable in the dissolution range 800 … 1000°C. It can be assumed that volatile compounds introduced with graphite are more effective towards ***a*** than the graphite itself, which is rather well conducting.

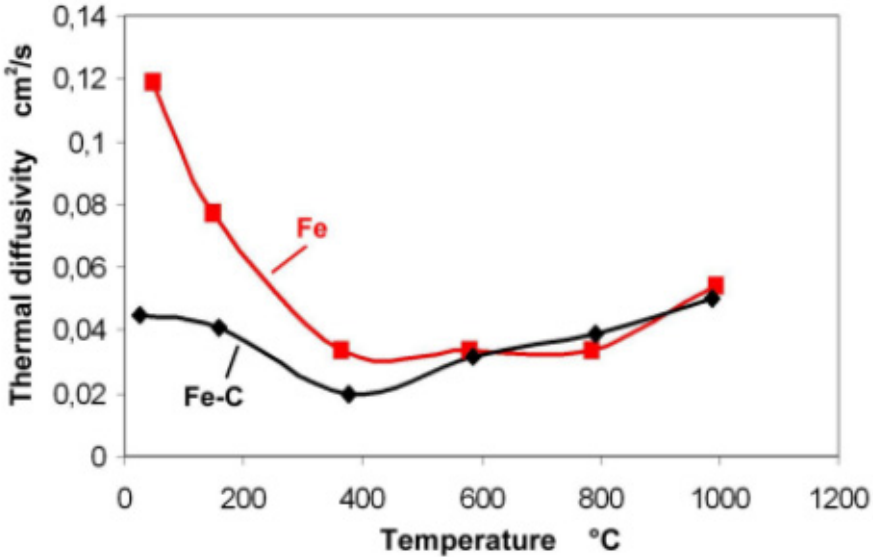

a) Heating section

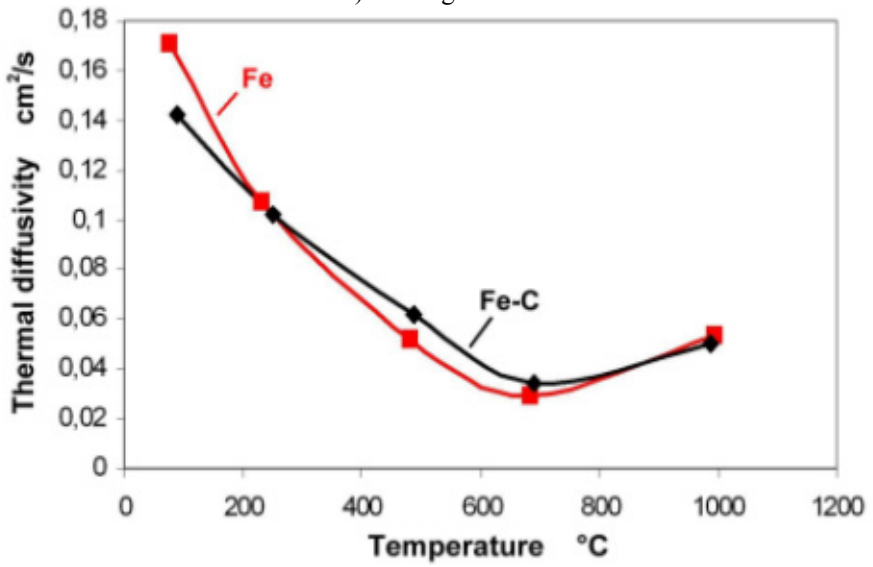

b) Cooling section

Fig.7. In-situ thermal diffusivity of Fe and Fe-0.8%C as a function of the temperature during a sintering run up to 1000°C.

From the cooling sections (Fig.7b) can be concluded that the effect both of dissolved carbon (in the austenite range) and of cementite on the thermal diffusivity is rather minor since both graphs coincide; only close to room temperature the plain iron material shows a slightly better ***a*** value. This agrees with the findings shown in [28] that at higher temperatures the porosity rather than the alloy elements affect thermal and electrical conductivity. In any case, the transport capacity of the sintering contacts for heat seems to be very similar for both materials. Here it should be considered that while the conductivity

of the matrix might be slightly lowered by the presence of carbon (dissolved or as Fe_3C) the effect of sintering will be somewhat more pronounced in Fe-C since the maximum sintering temperature applied here (1000°C = 1273 K) is 70% of the absolute solidus temperature for Fe compared to 77% for Fe-C, i.e. for Fe-C the sintering effect will be slightly more pronounced.

Including also the alloyed steels in the comparison (Fig.8) confirms that at room temperature it is mostly the graphite that influences the thermal diffusivity; in the heating section the graphs for Fe-Mo-C and Fe-Cr-Mo-C show a very similar behavior as Fe-C, just at a slightly lower level. At temperatures >600°C the Cr-Mo prealloyed steel differs from the other materials insofar as the increase of the diffusivity starts at 800°C compared to 600°C for the others, which, as stated already above, is an indicator of the stable surface oxides covering the Cr prealloyed powders. As shown e.g. in [34] it is the temperature range between 400 and 600°C within which the thin iron oxide layers initially covering the Cr-Mo steel powders [35] are transformed into more stable oxides than inhibit sintering ("internal getter" effect). Not the stable oxides themselves (which are still very thin) but their adverse effect on sintering is responsible for the slower increase of ***a*** with this material. For this type of steel, 1000°C is rather a low sintering temperature anyhow since the oxide layers just start to be carbothermally reduced [21], which explains why the a value for Fe-Cr-Mo-C recorded at 1000°C is lower than for the other steel grades.

The cooling section, in contrast, shows that this difference is virtually eliminated during cooling; at about 700°C rather identical thermal diffusivity values are measured for all the materials tested here. Only below 400°C the effect of the alloy elements becomes noticeable, the graphs for the alloyed steels deviating from those for Fe and Fe-C. This once more confirms that the effect of alloying elements on thermal diffusivity and conductivity is quite pronounced at and near room temperature but tends to virtually disappear at higher temperatures [28].

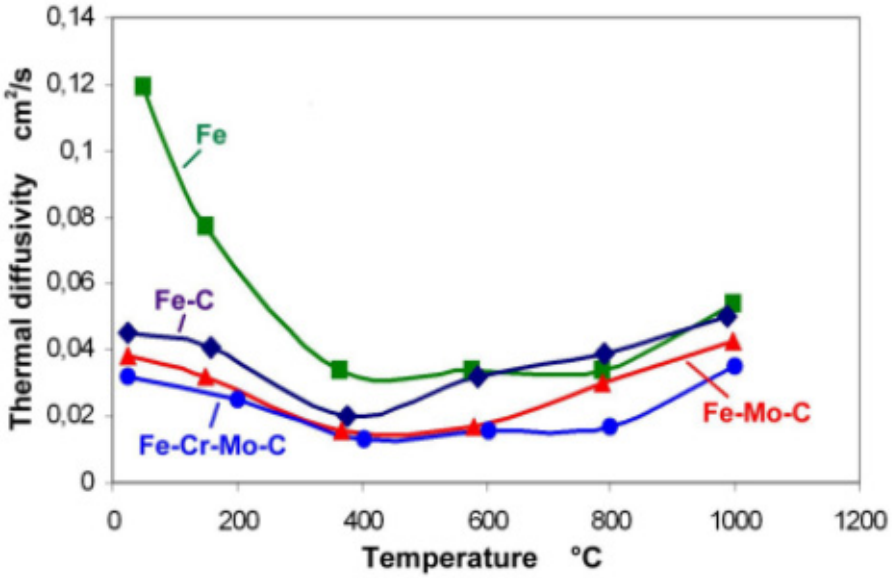

a) Heating section

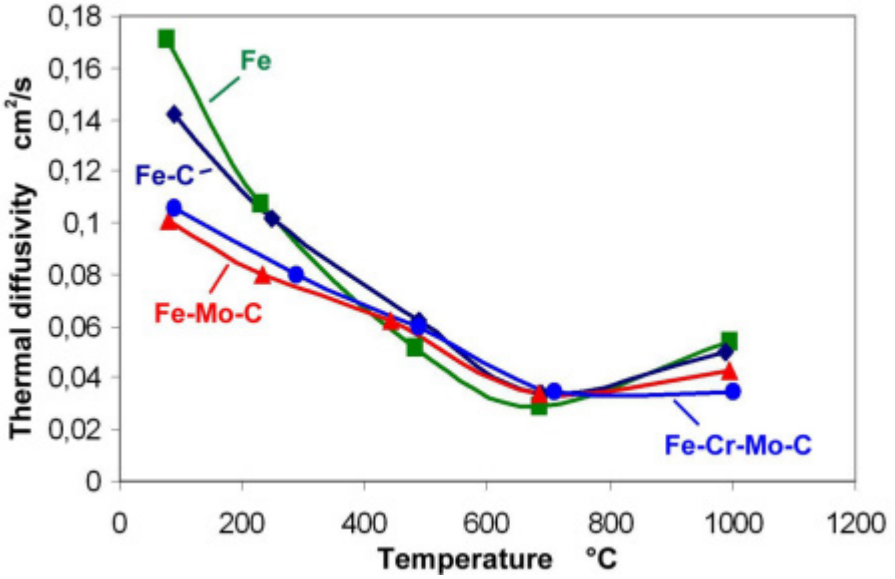

b) Cooling section

Fig.8. In-situ thermal diffusivity of different ferrous powder compacts as a function of the temperature during a sintering run up to 1000°C.

CONCLUSIONS

- In-situ measurement of the thermal diffusivity ***a*** during a simulated sintering run can be done by using the laser flash method. If the tests are done in vacuum, also porous powder compacts can be measured without undesirable interaction with the atmosphere.
- By carrying out test runs with plain iron compacts up to 1000°C it could be shown that the main changes occurring in the material that noticeably affect ***a*** occur at rather low temperatures, as evident when comparing the heating and the cooling sections. The cooling run yields virtually the same graph as does the second run in both heating and cooling. This indicates that the relevant processes are virtually temperature controlled, and the stepwise heating necessary with laser flash tests should not affect the results compared to constant heating rates.
- Carbon added as graphite results in lower initial diffusivity but on the other hand in a lower drop of ***a*** during heating. This can be attributed to the poor thermal conductivity of graphite compared to metal but on the other hand to the beneficial removal of volatile compounds in the early sintering stages.
- Alloy steels prepared from prealloyed powders result in quite similar heating graphs as does Fe-C, however the ***a*** levels are slightly lower. Esp. with Cr alloyed material the increase of ***a*** commonly observed in the temperature range 600…1000°C takes place only closely below the maximum temperature, i.e. above 800°C, indicating that the higher temperatures necessary for surface reduction in this material affect the formation of sintering contacts.
- In the cooling sections the materials differ only insignificanrly down to about 400°C; below this temperature the alloy steels show progressively lower ***a*** with decreasing temperature while the graphs for Fe and Fe-C separate only below 200°C, indicating

that the effect of C – as cementite – is less pronounced than that of metallic alloy elements such as Cr or Mo.

- Generally, the change of a during sintering is markedly less pronounced with ferrous compacts than with e.g. hard metals, due to the much lower change of the total porosity which in hard metals virtually disappears while in ferrous compacts it is only marginally reduced.
- From the values for the thermal diffusivity the thermal conductivity λ can be calculated which in turn can be used to calculate the electrical resistivity κ using Wiedemann-Franz' law for the λ-κ relationship. If this is done and the results are compared with resistivity data from previous investigations it is found that at least for plain iron the initial resistivity, i.e. that calculated from the green compact, is much too low while the final one, after the test run, is in excellent agreement with the experimentally obtained resistivity values. This indicates that in the initial stage the particle contacts are predominantly non-metallic, and thus Wiedemann-Franz' law cannot be applied, while after the test run metallic contacts are present for which the λ-κ relationship can be successfully used.

REFERENCES

[1] German, RM.: Int. J. Powder Metall., vol. 38, 2002, no. 2, p. 48
[2] Schatt, W: Sintervorgänge. Düsseldorf : VDI-Verlag, (1992
[3] Leitner, G., Jaenicke-Roessler, K., Gestrich, T., Breuning, T.: Metal Powder Report, vol. 52, 1999, no. 12, p. 32
[4] Gierl-Mayer, C., Danninger, H.: Powder Metall. Progress, vol. 15, 2015, no. 1, p. 3
[5] Shoales, GA.: P/M Sci. & Technol. Briefs, vol. 3, 2001, no. 1, p. 18
[6] Mousapour, M., Azadbeh, M., Danninger, H.: Powder Metallurgy, vol. 59**,** 2016, no. 5, p. 321
[7] Esper, FJ., Exner, HE., Metzler, H.: Powder Metall., vol. 18, 1975, p. 107
[8] Fortschritte der Pulvermetallurgie. Eds. F. Eisenkolb, F. Thümmler. Bd. 1. Berlin : Akademie-Verlag, 1963, p. 387
[9] Cytermann, R.: Powder Metall. Int., vol. 19, 1987, no. 1, p. 27
[10] Simchi, A., Danninger, H.: Powder Metall., vol. 43**,** 2000, no. 3, p. 209
[11] Simchi, A., Danninger, H., Weiss, B.: Powder Metall., vol. 43**,** 2000, no. 3, p. 219
[12] Simchi, A., Danninger, H., Gierl, C.: Powder Metall., vol. 44**,** 2001, no. 2, p. 148
[13] Schatt, W.: Powder Metall. Int., vol. 18, 1986, no. 1, p. 45
[14] Westphal, WH.: *Physik*, Springer-Verlag, Berlin-Göttingen-Heidelberg, 1959, p.314
[15] Raether, F., Springer, R.: Adv. Eng. Mater., vol. 2, 2000, no. 11, p. 741
[16] Danninger, H.: P/M Science & Technol. Briefs, vol. 1, 1999, no. 5, p. 19
[17] Danninger, H., Gierl, C., Leitner, G. In: Proc. 2000 Powder Metall. World Congress, Kyoto. Eds. K. Kosuge, H. Nagai. Part 2. The Japan Soc. of Powder and Powder Metall, 2001, p. 943
[18] Jangg, G., Drozda, M., Danninger, H., Schatt, W., Wibbeler, H.: Int. J. Powder Met. & Powder Techn., vol. 20, 1984, p. 287
[19] Danninger, H., Wolfsgruber, E., Ratzi, R. In: Proc. PM98 Granada. Vol. 2. Shrewsbury : EPMA, 1998, p. 290
[20] Danninger, H., Gierl, C.: J. Mater. Chem. & Physics, vol. 67, 2001, p. 49
[21] Kremel, S., Danninger, H., Yu, Y.: Powder Metall. Progress, vol. 2, 2002, no. 4, p. 211
[22] Netzsch Geraetebau, LFA 427 Data Sheet, Selb, D-95088 Selb / Germany
[23] Perl, M., Leitner, G: J. Thermal Analysis, vol. 47, 1996, p. 643
[24] Lehr, P.: C.R.Acad.Sci.France, vol. 242, 1956, p. 1172

[25] Kuroki, H., Suzuki, HY.: Mater. Transactions, vol. 47, 2006, p. 2449
[26] Danninger, H., Kremel, S., Leitner, G., Jaenicke-Roessler, K., Y,u Y.: Powder Metall. Progress, vol. 2, 2002, no. 3, p. 125
[27] Kremel, S., Raab, C., Danninger, H. In: Proc. EuroPM2001 Nice. Vol. 1. Shrewsbury: EPMA, 2001, p. 52
[28] Danninger, H., Gierl, C., Mühlbauer, G., Silva Gonzalez, M., Schmidt, J., Specht, E.: Int. J. Powder Metall., vol. 47, 2011, no. 3, p. 31
[29] Gille, G., Leitner, G., Roebuck, B. In: Proc. Europ. Conf. Adv. Hard Metals Prod., Stockholm. Shrewsbury : EPMA, 1996, p. 195
[30] Leitner, G.: J. Thermal Analysis and Calorimetry, vol. 56, 1999, p. 455
[31] Handbuch der Sonderstahlkunde. Ed. Houdremont. 3rd ed. Springer, 1956
[32] Thermophyikalische Stoffgrößen. Ed. W. Blanke. Springer, 1989
[33] Danninger, H., Frauendienst, G., Streb, KD., Ratzi, R.: Mater. Chemistry & Physics, vol. 67, 2001, p. 72
[34] Gierl-Mayer, C., de Oro Calderon, R., Danninger, H.: JOM, vol. 68, 2016, no. 3, p. 920
[35] Karlsson, H., Nyborg, L., Berg, S., Yu, Y. In: Proc. EuroPM2001, Nice. Vol. 1. Shrewsbury : EPMA, 2001, p. 22

Appendix: List of symbols

a …… thermal diffusivity [$cm^2.s^{-1}$]
c_p ….. Specific heat, at constant pressure; [$J.mole^{-1}.K^{-1}$]
κ …… electrical conductivity [$\Omega^{-1}.m^{-1}$]
λ …… thermal conductivity [$W.m^{-1}.K^{-1}$]
ρ …… density [$g.cm^{-3}$]